STEM CELLS®

TISSUE-SPECIFIC STEM CELLS

Bone Marrow-Derived Mesenchymal Stem Cells Promote Neuronal Networks with Functional Synaptic Transmission After Transplantation into Mice with Neurodegeneration

JAE-SUNG BAE,[a,b,c] HYUNG SOO HAN,[a] DONG-HO YOUN,[d] JANET E. CARTER,[b] MICHEL MODO,[e] EDWARD H. SCHUCHMAN,[f] HEE KYUNG JIN[c,g]

Departments of [a]Physiology, College of Medicine, [d]Oral Physiology, School of Dentistry and Brain Korea 21, [g]Laboratory Animal Medicine, College of Veterinary Medicine, and [c]Stem Cell Neuroplasticity Research Group, Kyungpook National University, Daegu, Korea; [b]Department of Mental Health Sciences, Royal Free and University College Medical School, University College London, London, United Kingdom; [e]Neuroimaging Research Group P042, Department of Neurology, Institute of Psychiatry, King's College London, London, United Kingdom; [f]Department of Human Genetics and Carl C. Icahn Institute for Gene Therapy and Molecular Medicine, Mount Sinai School of Medicine, New York, New York, USA

Key Words. Neural network by stem cells

ABSTRACT

Recent studies have shown that bone marrow-derived MSCs (BM-MSCs) improve neurological deficits when transplanted into animal models of neurological disorders. However, the precise mechanism by which this occurs remains unknown. Herein we demonstrate that BM-MSCs are able to promote neuronal networks with functional synaptic transmission after transplantation into Niemann-Pick disease type C (NP-C) mouse cerebellum. To address the mechanism by which this occurs, we used gene microarray, whole-cell patch-clamp recordings, and immunohistochemistry to evaluate expression of neurotransmitter receptors on Purkinje neurons in the NP-C cerebellum. Gene microarray analysis revealed upregulation of genes involved in both excitatory and inhibitory neurotransmission encoding subunits of the ionotropic glutamate receptors (α-amino-3-hydroxy-5-methyl-4-isoxazolepropionic acid, AMPA) GluR4 and $GABA_A$ receptor β2. We also demonstrated that BM-MSCs, when originated by fusion-like events with existing Purkinje neurons, develop into electrically active Purkinje neurons with functional synaptic formation. This study provides the first in vivo evidence that upregulation of neurotransmitter receptors may contribute to synapse formation via cell fusion-like processes after BM-MSC transplantation into mice with neurodegenerative disease. STEM CELLS *2007;25:1307–1316*

Disclosure of potential conflicts of interest is found at the end of this article.

INTRODUCTION

The therapeutic potential of bone marrow-derived MSC (BM-MSC) grafting has recently been studied in various pathological conditions of the central nervous system (CNS) [1–7]. Investigations have shown that BM-MSCs can give raise to Purkinje neurons in the cerebellum of adult human and normal mice [8, 9]. For example, Alvarez-Dolado et al. [10] and Weimann et al. [9] independently demonstrated that bone marrow-derived stem cells fuse with adult normal mouse Purkinje neurons when transplanted [9, 10]. Our recent studies also supported the idea that BM-MSC transplantation can be an effective therapeutic vehicle to deliver genetic material to Purkinje neurons via cell fusion [11–13]. Also, we have shown that neurodegenerative, pathological conditions may augment the ability of transplanted BM-MSCs to fuse with Purkinje neurons, although the mechanism by which BM-MSC-derived neurons mature and become functional remains unknown [13].

Recent advances in stem cell technology have led to purification and in vitro propagation of stem cells from embryonic and adult tissues of various species, including humans [14, 15]. Several groups have isolated adult cells whose progeny express neuronal antigens, in vivo and in vitro [16–20]. Rarely addressed, however, is the question of whether adult stem cells can give rise to fully differentiated and functional neurons in vivo. It is not yet known whether adult stem cell-derived neurons have even basic functional properties of mature CNS neurons, such as action potential activity [16–19]. Mature CNS neurons are polarized, normally with a single axon and multiple dendrites. They are able to communicate with other cells by releasing and detecting neurotransmitters at their synapses. A few studies have reported that neurons derived from adult progenitor cells show rather limited neuronal maturation in vitro, as evidenced by small voltage-dependent Na^+ currents [20] and the efficient formation of synapses [21]. It is not clear whether the neural progeny of adult stem cells retain the ability to respond to neuronal maturation and synapse formation when they are trans-

Correspondence: Hee Kyung Jin, D.V.M., Ph.D., College of Veterinary Medicine, Kyungpook National University, Daegu 702-701, Korea. Telephone: 82-53-950-5966; Fax: 82-53-950-5955; e-mail: hkjin@mail.knu.ac.kr Received September 4, 2006; accepted for publication January 25, 2007. ©AlphaMed Press 1066-5099/2007/$30.00/0 doi: 10.1634/stemcells.2006-0561

planted into mammals. Here, we established an in vivo system to examine the functional potential of neural progeny of BM-MSCs in Niemann-Pick disease type C (NP-C) mice. BALB/c npc^{nih} (NP-C) mice, a model of human Niemann-Pick disease type C1, undergo a characteristic pattern of Purkinje neuron loss, increasing from lobe I of the anterior zone to lobe VII of the posterior cerebellar vermis [22]. Our study has provided the first in vivo evidence that upregulation of synaptic transmission-related genes following a BM-MSC/Purkinje cell fusion-like event may contribute to the alleviation of functional neurodegenerative deficits in mice. Moreover, these findings provide the first insights into the molecular mechanism(s) that promote the BM-MSC/Purkinje neuron fusion-like process and may lead to the development of better therapeutic approaches for preventing Purkinje neuron loss in various neurodegenerative diseases.

MATERIALS AND METHODS

Animals

All animal husbandry procedures performed were in accordance with the guidelines of the Laboratory Animal Care and Use Committee of the College of Veterinary Medicine, Kyungpook University. A colony of BALB/c npc^{nih} (NP-C) mice was maintained, and the genotype of each mouse was determined by polymerase chain reaction (PCR) [23]. The NP-C $Gsbs^{GFP/+}$ mice were created by crossing NP-C mice with $Gsbs^{GFP/+}$ mice, which carry a null allele of *Gsbs* (GenBank accession number MGI:1333876) on BALB/c background and concomitantly have the green fluorescent protein (GFP) reporter gene inserted into the *Gsbs* locus [13, 24].

Isolation and Culture of MSCs

Tibias and femurs were dissected from 6- to 8-week-old normal mice in the NP-C colony and heterozygous *Phgdh-DsRed2* mice [13]. Bone marrow was harvested, and single-cell suspensions were obtained using a 40-μm cell strainer (Becton, Dickinson and Company, Franklin Lakes, NJ, http://www.bd.com). Approximately 10^7 cells were plated in 75-cm^2 flasks containing MyeloCult M5300 culture medium (Stem Cell Technologies, Vancouver, BC, Canada, http://www.stemcell.com) with antibiotics, according to our previous reports [11, 12]. To obtain MSC, the cells were grown for 2 weeks, and the plastic-adherent population (i.e., MSCs) was used. Most adherent cells expressed CD29 and CD90 (supplemental online Fig. 1). In contrast, the majority of adherent cells were negative for CD34, CD45, and CD117. A small fraction of adherent cells expressed CD71.

Cell Transplantation

NP-C and NP-C $Gsbs^{GFP/+}$ mice (approximately 3 weeks of age; $n = 30$ of each genotype) were anesthetized with a combination of 100 mg/kg ketamine and 10 mg/kg xylazine and injected using the Styrofoam platform of a stereotaxic injection apparatus (Stoelting Co., Wood Dale, IL, http://www.stoeltingco.com) as described [13]. To determine whether the result after BM-MSC transplantation is directly attributable to a specific cell, we used NIH 3T3 cells as a non-stem cell control condition. BM-MSCs that expressed donor-derived DsRed2 protein and NIH 3T3 cells that were labeled with the membrane-bound fluorescent marker PKH26 (Sigma-Aldrich, St. Louis, http://www.sigmaaldrich.com) were transplanted into the cerebellum using a glass capillary (1.2 × 0.6 mm) [12]. The injection coordinates were 5.52 mm posterior to bregma, and injection depth was 2.50 mm. Each recipient received approximately 1×10^6 cells in 3 μl of cell suspension at a rate of 0.15 μl/minute. For sham transplantation, animals underwent the same transplantation procedure but received a vehicle infusion of an equal volume of Hanks' balanced saline solution. After transplantation, the scalp was closed by suture, and the animals recovered from the anesthesia before they were returned to their cage. Age-matched normal littermates in the NP-C colony were used as controls.

Microarray Analysis

Brain tissues slices of cerebellar injection sites were prepared from BM-MSC-, NIH 3T3 cell-, and sham-transplanted NP-C mice 2 and 4 weeks after transplantation or sham transplantation. Three individual animals were analyzed per group for each condition and pooled together for reverse transcription. Total RNA was isolated using RNeasy Midi kit (Qiagen, Valencia, CA, http://www1.qiagen.com) according to the manufacturer's protocol, followed by further purification using the Oligotex Midi kit (Qiagen). Twenty micrograms of RNA from each sample were used for synthesis of cDNA, followed by labeling of the cRNA with biotin. The labeled target cRNA was fragmented and hybridized to the GeneChip Mouse Genome 430 2.0 Array (Affymetrix, Santa Clara, CA, http://www.affymetrix.com). The chip contains 45,000 probe sets for more than 39,000 transcripts, variants from more than 39,000 transcripts, and variants from more than 34,000 well-characterized mouse genes. Hybridization and scanning were carried out by the Seoulin Molecular Biology Technique Center in Korea, with the Affymetrix Fluidics Station and GeneChip Scanner 3000 enabled for high-resolution scanning and the GeneChip operating software with the GeneChip Scanner 3000 high-resolution scanning patch. Data acquisition was performed using the Affymetrix Microarray Suite, and the data were analyzed with dChip [25] and GenMAPP tools [26, 27]. Statistical analyses were performed using dChip software (Student's t test; significance level set at $p < .05$).

Quantitative Real-Time PCR

To validate the microarray data, a select number of differentially expressed genes were chosen for quantitative real-time PCR. The RNA samples from total of three individual animals per group in the different experiment were used to prepare cDNA for reverse transcription-PCR using the Moloney murine leukemia virus reverse transcriptase (Promega, Madison, WI, http://www.promega.com). The cDNA was quantified using the QuantiTect SYBR Green PCR kit (Qiagen) and the LightCycler (Roche Diagnostics, Basel, Switzerland, http://www.roche-applied-science.com). The PCR primers used were as follows: GluR4 forward, 5′-GCTGCAGCTAAGACCTTCACTG-3′; GluR4 reverse, 5′-CCCCTGTCTGTATCATACAGGAAGA-3′; $GABA_A$ $\beta 2$ forward, 5′-CCACATCCGAAGCAGTAATGGG-3′; $GABA_A$ $\beta 2$ reverse, 5′-TGCTGGAGGCATCATAGGC-3′. For each transcript investigated, a mixture of the following reaction components was prepared to the indicated end concentration: $MgCl_2$, 2.5 mM; forward primer, 0.4 μM; reverse primer, 0.4 μM; and QuantiTect SYBR Green PCR Master mix (Qiagen). The 9 μl of Master mix was filled in the glass capillaries, and a 1-μl volume, containing 25 ng of reverse-transcribed total RNA, was added as PCR template. Capillaries were closed, centrifuged, and placed into the LightCycler rotor. The real-time PCR primers and experimental protocol for each gene was designed according to previous reports [28–30].

SDS–Polyacrylamide Gel Electrophoresis and Immunoblotting

Brain samples were homogenized in Laemmli lysis buffer plus protease inhibitors. Aliquots containing 30 μg of protein were subjected to 10% SDS-polyacrylamide gel electrophoresis. Protein bands were transferred to polyvinylidene difluoride membrane (Millipore, Billerica, MA, http://www.millipore.com) and probed by incubating in the primary antibodies, followed by a horseradish peroxidase-conjugated secondary antibody (1:5,000; Santa Cruz Biotechnology Inc., Santa Cruz, CA, http://www.scbt.com). We used the primary antibodies raised against GluR1, GluR2/3, GluR4 (1:500; Upstate, Charlottesville, VA, http://www.upstate.com), and $GABA_A$ receptor $\beta 2$ (1:1,000; Chemicon, Temecula, CA, http://www.chemicon.com). To determine the specificity of the primary antibodies, we used antibodies preabsorbed with blocking peptides instead of primary antibodies. Blots were visualized using the ECL

Table 1. The number of genes that showed changes in gene expression in BM-MSC-transplanted Niemann-Pick disease type C brain tissue compared with controls

	2 Weeks after BM-MSC transplantation		4 Weeks after BM-MSC transplantation	
	Increased	Decreased	Increased	Decreased
1.2-fold	2,579	2,522	3,116	2,351
1.5-fold	1,060	930	1,586	806
2.0-fold	59	7	369	187

Abbreviation: BM-MSC, bone marrow-derived MSC.

system (Amersham Biosciences, Piscataway, NJ, http://www.amersham.com) according to the manufacturer's directions and exposed to x-ray film. Equal protein loading was confirmed by measuring β-actin (1:5000; anti-β-actin; Sigma-Aldrich). Densitometric measurements were made from the film using an imaging densitometer (Bio-Rad, Hercules, CA, http://www.bio-rad.com) and then quantified using Bio-Rad analysis software. For quantification of relative protein expression, the optical density of the protein band of interest was normalized to the optical density of β-actin on the same gel.

Electrophysiology

Parasagittal slices of the cerebellar mediolateral vermis (250 μm thick) were prepared from BM-MSC-transplanted NP-C $Gsbs^{GFP/+}$ and BALB/c $Gsbs^{GFP/+}$ mice using a vibrating tissue slicer and ice-cold Krebs solution (composition: 117 mM NaCl, 3.6 mM KCl, 2.5 mM $CaCl_2$, 1.2 mM $MgCl_2$, 1.2 mM NaH_2PO_4, 25 mM $NaHCO_3$, and 11 mM glucose; preoxygenated with 95% O_2/5% CO_2 at pH 7.4). Whole-cell recordings were then obtained from the identified fluorescent cells expressing GFP and/or DsRed in the Purkinje layer of the parasagittal slices (cerebellar lobe IV–VI) under an infrared differential interference contrast system with appropriate filter and mirror units (U-MWIB2 for GFP and U-MWIG2 for DsRed; Olympus, Tokyo, http://www.olympus-global.com) and performed using patch pipettes (TW150F-4; World Precision Instruments, Sarasota, FL, http://www.wpiinc.com) with a resistance of 8–10 MΩ when filled with internal solution (composition: 135 mM K-gluconate, 0.5 mM $CaCl_2$, 2 mM $MgCl_2$, 5 mM KCl, 5 mM EGTA, 5 mM HEPES, 5 mM Na_2ATP). Cells in the whole-cell configuration were voltage-clamped at a holding potential of −70 mV to record spontaneous excitatory postsynaptic currents (sEPSCs) and current-clamped to record action potentials by various steps of intracellular current injections. The responses were amplified by Multiclamp 700A (Axon Instruments/Molecular Devices Corp., Union City, CA, http://www.moleculardevices.com), sampled at 10 kHz (Digidata 1320; Axon Instruments), and low-pass-filtered at 2 kHz. After each recording was finished, the recorded cell was photographed using charge-coupled device camera ($CoolSNAP_{HQ}$; Photometrics, Tucson, AZ, http://www.photomet.com) under each filter cube for GFP or DsRed excitation and emission wavelengths. sEPSCs were picked manually and analyzed using pClamp software (version 9.2; Axon Instruments). One to three neurons were recorded in each slice.

Histological Analysis

Transplanted mice were sacrificed at 2 and 5 weeks after transplantation by cardiac perfusion, and tissues were collected and frozen. Frozen sections (15 μm) were then prepared for fluorescent immunostaining. For immunohistochemistry, primary antibodies against calbindin D28K (rabbit; 1:500; Chemicon) were used. After incubation, the slides were washed and incubated with Alexa Fluor 488 (Molecular Probes Inc., Carlsbad, CA, http://probes.invitrogen.com). For filipin and sphingomyelin staining, analyses were carried out as previously described [13, 31, 32]. The sections were analyzed by use of a fluorescent microscope (Olympus BX51).

Accelerating Rota-Rod Analysis

The Rota-Rod test assesses an animal's balance and coordination by measuring the amount of time the animal is able to remain on a longitudinally rotating rod. The Rota-Rod apparatus (accelerating model 47600; Ugo Basile, Comerio, Italy, http://www.ugobasile.com) [33] has a 3-cm-diameter rod, suitably machined to provide grip. In this apparatus, a motor sets the rotor in motion via the gear belt at a selected speed. When the mouse falls off its cylinder section, the plate below trips, and the corresponding counter is disconnected, thereby recording the animal's endurance time in seconds. Use of an accelerating model ensures that screening results are less scattered [34]. The machine was set to an initial speed of 32 rpm, and the acceleration was increased by 32 rpm every 25–30 seconds. Transplanted NP-C mice were analyzed along with sham-transplanted NP-C and normal control mice. Scores were registered every week (at least three independent tests were performed for each time point) beginning 1 week after transplantation. Uniform conditions were carefully maintained for each test, and there was a rest time of 1 hour between trials. A maximum time limit of 300 seconds per test was established. Data were analyzed using a one-tailed Student t test, and comparisons were made between the transplanted and control groups.

Magnetic Resonance Imaging

Perfusion-fixed total brains were isolated from BM-MSC, sham-transplanted NP-C, and normal mice (3 weeks after transplantation). ^1H magnetic resonance imaging (MRI) was performed using a 4.7 Tesla superconducting magnet (Oxford Instruments, Abingdon, U.K., http://www.oxford-instruments.com) interfaced to a UNITY Inova-200 imaging console (Varian, Palo Alto, CA, http://www.varianinc.com) and a 40-mm internal diameter quadrature birdcage radiofrequency coil (Varian). Magnetic resonance image acquisition consisted of a gradient echo sequence (repetition time, 2.4 seconds; echo time, 15 ms; number of averages, 14; matrix, 256 × 256; field of view, 1.28 × 1.28 cm; number of slices, 50; slice thickness, 0.3 mm; in-plane resolution, 0.1 × 0.1 mm; acquisition time, 1 hour 22 minutes 19 seconds). Raw data were converted to the University of North Carolina format using in-house software. For volume measurements, the total number of delineated pixels was calculated using the xdispunc program (version 4.9; Dave Plummer, University College London/London, U.K.). The total number of pixels per slice was then multiplied by the spatial resolution of the scan to produce volume measurements per image slice.

Statistical Analysis

Statistical differences among groups were analyzed by use of the Tukey honestly significant difference test and the repeated measures analysis of variance test by the SAS statistical package (release 8.1; SAS Institute Inc., Cary, NC, http://www.sas.com). $p < .05$ was considered to be significant.

Results

Elevation of Genes Associated with Neurotransmitters After BM-MSC Transplantation

For gene expression analyses of the brain, we used NP-C animals 2 and 4 weeks after BM-MSC and NIH 3T3 cell transplantation and, as controls, age-matched, sham-transplanted NP-C mice. As expected, transplantation caused marked alterations in the expression levels of many genes. To observe the general transcriptional activity, we measured the changes in expression level of a numbers of genes (Table 1). A total of 5,101 genes at 2 weeks and 5,467 genes at 4 weeks after BM-MSC transplantation (from 45,000 genes on the chip) showed more than 1.2-fold change. Using an arbitrary cut-off of 2.0-fold change, 59 genes at 2 weeks and 369 at 4 weeks after

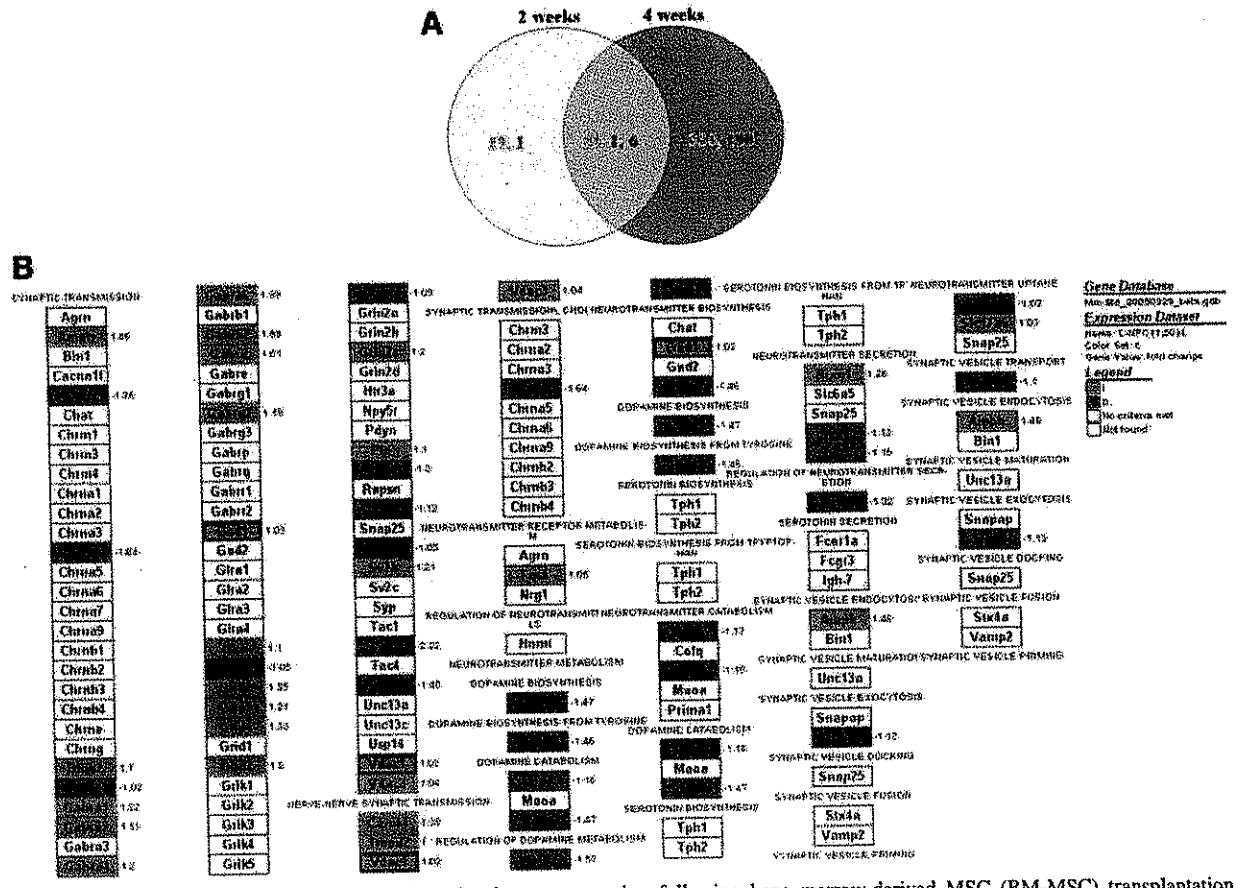

Figure 1. The changes in synaptic transmission-related gene expression following bone marrow-derived MSC (BM-MSC) transplantation in Niemann-Pick disease type C (NP-C) mice. **(A):** Venn diagram showing transcript distribution at 2 and 4 weeks after BM-MSC transplantation. The results indicate that 46 gene transcripts overlap. Of note, 39 genes showed upregulated expression, and six genes showed downregulated expression at both 2 and 4 weeks after BM-MSC transplantation; only one gene showed a different expression pattern. The diagram was generated from list of transcripts that are >2.0-fold enriched, relative to sham-transplanted NP-C. **(B):** The changes in synaptic transmission-related gene expression at 2 weeks after BM-MSC transplantation. The genes in red are upregulated and genes in blue are downregulated compared with sham-transplanted NP-C. Some of GABA receptors (Gabra) and AMPA receptors (Gria) showed increased gene expression. This figure was made with the freely accessible software GenMAPP tools. Abbreviations: CHOL, choline; D, decrease; I, increase.

BM-MSC transplantation showed increased expression (Table 1). From the genes enriched by the absolute value of fold change >2.0, Venn diagrams were constructed to display the proportions of transcripts shared between 2 and 4 weeks after BM-MSC transplantation. The results indicate that 46 genes overlap at these time points. Of note, 39 genes showed upregulated expression and 6 genes showed downregulation at both 2 and 4 weeks after BM-MSC transplantation. Only one gene showed upregulated expression at 2 weeks but downregulation at 4 weeks after BM-MSC transplantation (Fig. 1A).

We next identified individual genes from overlapping of upregulated 39 at both time points. Most of the overlapped genes were attributed to cell signaling and general cellular activities. Of these genes, interestingly, BM-MSC-transplanted NP-C mice showed induction of several synaptic transmission-related genes. For the preliminary analysis, it was decided to concentrate further only on genes that are specifically upregulated and on those thought to have a particular role in relation to synaptic transmission. α-Amino-3-hydroxy-5-methyl-4-isoxazolepropionic acid (AMPA) and GABA receptor subtypes were significantly upregulated at both 2 and 4 weeks after BM-MSC transplantation. Myelin and glutamate decarboxylase (GAD) showed slightly upregulation at both 2 and 4 weeks in BM-MSC-transplanted NP-C brain (Fig. 1B). All of these genes have been implicated in other studies [29, 35–37] in neurotransmission in the cerebellum.

To validate whether the gene expression profile in this experiment is stem cell-specific, we transplanted NIH 3T3 cells (non-neuronal cells with BM-MSC-like morphology) instead of BM-MSCs into NP-C mice as an appropriate control and performed microarray analysis. Of note, the expression profile of genes involved in synaptic transmission in NIH 3T3 cell-transplanted NP-C mice was different from that of BM-MSC-transplanted NP-C mice (supplemental online Fig. 2; Table 2). Of 161 synaptic transmission-related genes, 40 genes were statistically significant from the control group ($p < .05$). The specific expression level of 40 genes was compared between NIH 3T3 cell-transplanted and BM-MSC-transplanted conditions. Most of the genes showed a clear differential effect in the NIH 3T3-transplanted NP-C mice compared with BM-MSC-transplanted NP-C mice (Table 2).

We performed quantitative real-time PCR on a select number of these genes to validate the microarray findings. Among the many subunits of AMPA receptors, GluR4 had significantly increased expression at 2 weeks after BM-MSC transplantation, but it returned to basal level at 4 weeks after BM-MSC transplantation. The absolute level of expression of

Table 2. From the genes in Figure 1, genes with a statistically significant increase ($p < .05$) were compared in BM-MSC-transplanted Niemann-Pick disease type C (NP-C) and NIH 3T3 cell-transplanted NP-C brain tissues

Abbreviation	Gene name	GenBank accession no.	Fold change	
			BM-MSC	NIH 3T3
Agrn	Agrin	MGI:87961	1.06	1.65
Bin1	Bridging integrator 1	MGI:108092	1.1	1.84
Cacna1f	Cocaine and amphetamine regulated transcript	MGI:1351330	−1.29	−1.53
Chat	Choline acetyltransferase	MGI:88392	−1.02	−2.01
Chrna3	Cholinergic receptor, nicotinic, α-polypeptide 3	MGI:87887	−1.03	1.97
Chrna6	Cholinergic receptor, nicotinic, α-polypeptide 6	MGI:106213	−1.5	−1.6
Chrna9	Cholinergic receptor, nicotinic, α-polypeptide 9	MGI:1202403	−1.18	1.35
Chrnb4	Cholinergic receptor, nicotinic, β-polypeptide 4	MGI:87892	1.08	1.51
Chrng	Cholinergic receptor, nicotinic, γ polypeptide	MGI:87895	−1.01	2.45
Dlgh2	Discs, large homolog 2 (*Drosophila*)	MGI:1344351	1.14	−1.62
Gabra3	$GABA_A$ receptor, subunit α 3	MGI:95651	1.01	−1.6
Gabra4	$GABA_A$ receptor, subunit α4	MGI:95616	1.05	−1.66
Gabrb2	$GABA_A$ receptor, subunit β2	MGI:95620	1.64	−2.13
Gabrd	$GABA_A$ receptor, subunit δ	MGI:95622	1.52	1.67
Gabre	$GABA_A$ receptor, subunit ϵ	MGI:1330235	1.59	−1.76
Gabrp	$GABA_A$ receptor, π	MGI:2387597	1.81	−1.82
Gabrr2	$GABA_C$ receptor, subunit ρ 2	MGI:95626	1.07	1.72
Glra2	Glycine receptor, α2 subunit	MGI:95748	−1.06	−1.74
Glra4	Glycine receptor, α4 subunit	MGI:95750	1.13	1.67
Gria3	Glutamate receptor, ionotropic, AMPA3 (α3)	MGI:95810	1.15	−1.9
Grid2	Glutamate receptor, ionotropic, δ2	MGI:95813	1.27	−2.19
Grik1	Glutamate receptor, ionotropic, kainate 1	MGI:95814	1.01	−3.12
Grik2	Glutamate receptor, ionotropic, kainate 2 (β2)	MGI:95815	1.1	−2.75
Grik5	Glutamate receptor, ionotropic, kainate 5 (γ2)	MGI:95815	−1.09	1.64
Grin2c	Glutamate receptor, ionotropic, NMDA2C (ϵ3)	MGI:95822	1.21	2.27
Grin2d	Glutamate receptor, ionotropic, NMDA2D (ϵ4)	MGI:95823	−1.03	1.82
Hir3a	5-Hydroxytryptamine (serotonin) receptor 3A	MGI:96282	−1.04	1.52
Plp	Proteolipid protein (myelin)	MGI:97623	1.11	−1.85
Pnoc	Prepronociceptin	MGI:105308	−1.32	−2.04
Rapsn	Receptor-associated protein of the synapse	MGI:99422	−1.16	1.76
Slc12a5	Solute carrier family 12, member 5	MGI:1862037	−1.05	1.89
Tac2	Tachykinin 2	MGI:98476	−2.25	−2.55
Vdac1	Voltage-dependent anion channel 1	MGI:106919	−1.08	−2.49
Nr4a2	Nuclear receptor subfamily 4, group A, member 2	MGI:1352456	−1.51	−2.65
Slc6a3	Solute carrier family 6 (neurotransmitter transporter, dopamine), member 3	MGI:94862	−1.48	−1.82
Tph2	Tryptophan hydroxylase 2	MGI:2651811	−1.05	−2.63
Slc6a5	Solute carrier family 6 (neurotransmitter transporter, glycine), member 5	MGI:105090	1.1	2.16
Fcer1a	Fc receptor, IgE, high affinity I, α-polypeptide	MGI:95494	1.08	2.52
Trim9	Tripartite motif protein 9	MGI:2137354	−1.13	−1.89
Vamp2	Vesicle-associated membrane protein 2	MGI:1313277	1.04	2.55

Abbreviation: BM-MSC, bone marrow-derived MSC.

$GABA_A$ receptor β2 showed a pattern similar to that of GluR4 (Fig. 2A). GAD and myelin basal protein (MBP) were increased at 2 weeks after BM-MSC transplantation (supplemental online Fig. 3A), although expression of MBP did not reach statistical significance. We failed to confirm upregulation of GluR1, 2, and 3 in this quantitative analysis (data not shown).

To determine whether GluR1, GluR2, GluR3, GluR4, $GABA_A$ receptor β2, GAD, and MBP were produced at the protein level at 2 and 4 weeks after BM-MSC transplantation, we undertook Western blot analysis. These results confirm that GluR4 protein level is dramatically increased at 2 and 4 weeks after BM-MSC transplantation in NP-C mice compared with control sham-transplanted NP-C mice (Fig. 2B). Expression at the protein level for the GluR1, GluR2, GluR3, $GABA_A$, GAD, and MBP could not be confirmed by immunoblot analysis (data not shown), but immunofluorescent analysis for GluR1, 2, and 3 demonstrated strong expression in Purkinje neurons at 2 weeks after BM-MSC transplantation in NP-C mice (supplemental online Fig. 3B, 3C).

Electrophysiology of Purkinje Neurons in Transplanted NP-C *Gsbs*$^{GFP/+}$ Mice

To investigate whether surviving Purkinje neurons in the NP-C *Gsbs*$^{GFP/+}$ mice are electrically active and their synapses functional, we performed whole-cell patch-clamp recordings. In transplanted NP-C *Gsbs*$^{GFP/+}$, many surviving Purkinje neurons were doubled-labeled by both endogenous GFP and donor (MSC)-derived DsRed2 proteins. In GFP/DsRed-positive Purkinje neurons obtained from parasagittal slices of the transplanted mice, various numbers of action potential firings were triggered by intracellular injection of depolarizing current pulses (0.5–1.1 nA, 300 ms; Fig. 3A, lower left). In addition, sEPSCs (holding potential, −70 mV) were recorded in the GFP/DsRed-positive Purkinje neurons, although their frequencies were low and variable among neurons. In contrast to the GFP/DsRed-positive Purkinje neurons, neurons that were DsRed-positive only, which presumably originated from donor BM-MSCs that had differentiated rather than fused with existing neurons, had no action potential firing in current clamp and no sEPSC in voltage clamp (Fig. 3B). These results indicate that only GFP/

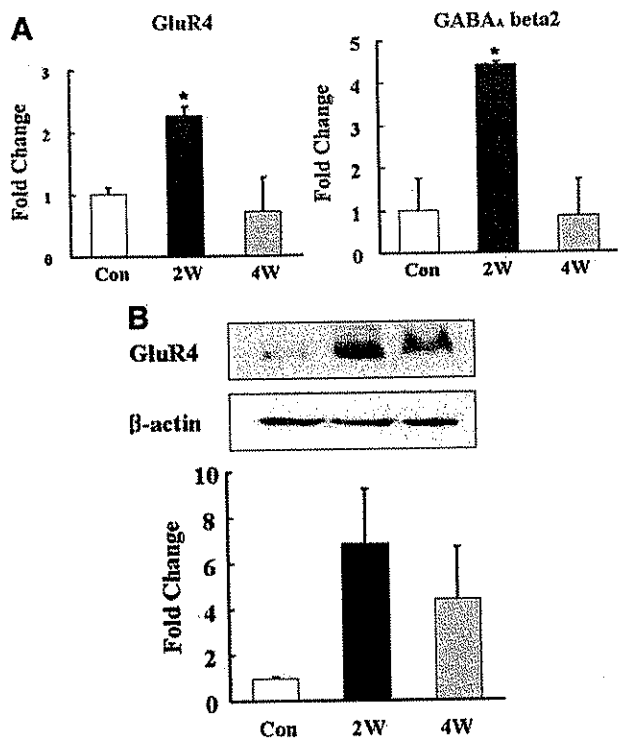

Figure 2. Bone marrow-derived MSC (BM-MSC) transplantation induced synaptic transmission related gene expression in Niemann-Pick disease type C (NP-C) mice ($n = 3$ in each group). **(A):** Gene expression of GluR4 and $GABA_A$ receptor β2 was quantitatively measured using real-time polymerase chain reaction. Black bars, 2W after BM-MSC transplantation; gray bars, 4W after BM-MSC transplantation; white bars, sham-transplanted NP-C mice. In the sham-transplanted NP-C brain, absolute level of GluR4 and $GABA_A$ receptor β2 was relatively lower than 2W after transplantation. The increase in GluR4 expression returned to basal levels at 4W after transplantation. BM-MSCs transplanted into NP-C brain at 2 weeks also showed enhanced gene expression of $GABA_A$ receptor β2. *, $p < .05$ versus Con. **(B):** Representative Western blot analysis shows increased expression of GluR4 at 2W and maintenance of high-level expression at 4W after BM-MSC transplantation. $GABA_A$ receptor β2 was hardly detectable in all conditions. *, $p < .05$ versus Con. Abbreviations: Con, control; 2W, 2 weeks; 4W, 4 weeks.

DsRed-positive Purkinje neurons that had originated from cell fusion-like events in the transplanted NP-C *Gsbs*$^{GFP/+}$ mice are electrically active and have functional synapses.

Furthermore, when we extended the recordings in NP-C *Gsbs*$^{GFP/+}$ mice to 4 weeks after transplantation, we found that some of GFP/DsRed-positive Purkinje neurons (Fig. 3C) showed sEPSCs as frequently as wild-type Purkinje neurons (Fig. 3D). The sEPSCs were not affected by the application of tetrodotoxin (TTX) (1 μM), a voltage-dependent Na^+ channel blocker, but were blocked by the addition of 6-cyano-7-nitroquinoxaline-2,3-dione (10 μM) to TTX, an AMPA/kainate receptor antagonist (Fig. 3C), indicating that the synaptic responses in the double-labeled Purkinje neurons (originating from cell fusion-like events) are mediated by glutamate receptors expressed at functional synapses of the neurons. As summarized in Figure 3E, the mean frequency of sEPSCs recorded in Purkinje neurons of NP-C *Gsbs*$^{GFP/+}$ mice at 4 weeks after transplantation ($GFP^+/DsRed^-$ Purkinje neurons, 0.92 ± 0.33 Hz, $n = 3$; $GFP^+/DsRed^+$ Purkinje neurons, 0.19 ± 0.03 Hz, $n = 5$; for all, 0.46 ± 0.17 Hz, $n = 8$) tended to recover to the value in BALB/c *Gsbs*$^{GFP/+}$ mice (0.87 ± 0.16, $n = 8$), whereas that in NP-C *Gsbs*$^{GFP/+}$ mice at 2 weeks after transplantation ($GFP^+/DsRed^-$ Purkinje neurons, 0.52 ± 0.13 Hz, $n = 4$; $GFP^+/DsRed^+$ Purkinje neurons, 0.18 ± 0.04 Hz, $n = 8$; for all, 0.29 ± 0.06 Hz, $n = 12$) was significantly decreased ($p < .01$ vs. wild-type). On the other hand, there was no significant difference among groups in sEPSC amplitude (Fig. 3E).

Improved Morphological Change, Cerebellar Function, and Anatomical Distribution in the BM-MSC-Transplanted NP-C Mice

NP-C mice undergo a characteristic pattern of Purkinje neuron loss, increasing from lobe I of the anterior zone to lobe VII of the posterior cerebellar vermis [22]. Purkinje neurons were quantified by immunohistochemistry using calbindin antibodies. Figure 4A shows representative sections from NP-C-transplanted (BM-MSCs and NIH 3T3 cells) and control (sham-transplanted NP-C and normal) mice at 2 and 4 weeks after transplantation. Note that an almost complete disappearance of Purkinje neurons was evident in the NIH 3T3 cell-transplanted and sham-transplanted NP-C mice, and there was extensive vacuolization. In contrast, the number of surviving Purkinje neurons was increased substantially in lobe VII of BM-MSC-transplanted NP-C mice (Fig. 4B; $p < .05$, transplanted vs. sham-transplanted groups). In addition, we identified many GFP/DsRed-positive Purkinje neurons (double nuclei, 20.6% of total), similar to findings reported in our previous study [13].

The Rota-Rod test assesses an animal's balance and coordination by measuring the amount of time the animal is able to remain on a longitudinally rotating rod. There were significant improvements in cerebellar function, as identified by Rota-Rod analysis, in BM-MSC-transplanted NP-C mice compared with the NIH 3T3 cell-transplanted and sham-transplanted NP-C mice (Fig. 4C).

We performed ex vivo MRI scans to investigate anatomical changes in the brain following BM-MSC transplantation in NP-C mice. Volumetric measurements of ex vivo MRI scans of perfusion-fixed animals revealed that for both BM-MSC-transplanted and sham-transplanted NP-C mice, overall brain size was approximately 10% smaller than that of normal mice. However, this atrophy did not reach statistical significance. (Fig. 4D). When focusing on the cerebellum, the primary site of pathology and transplantation, sham-transplanted NP-C mice have a brain volume approximately 60% smaller, which potentially could contribute to the smaller brain volumes observed. Although transplanted NP-C mice showed attenuation of cerebellar atrophy compared with sham-transplanted mice, this did not reach statistical significance, and cerebellar volume remained significantly smaller compared with normal mice (Fig. 4E, $p < .05$).

Analysis of Cholesterol and Sphingomyelin Levels in Transplanted NP-C Mice

In an attempt to correlate enhanced survival of Purkinje neurons with the outcome of NP-C pathologies, we evaluated the effect of the BM-MSC transplantation on intracellular accumulation of cholesterol and sphingomyelin by using specific probes. Filipin was used to stain for unesterified cholesterol [27, 28], and lysenin immunohistochemistry was applied for sphingomyelin detection [11, 28]. As shown in Figure 5, filipin and lysenin staining demonstrated that these lipids were markedly decreased in the Purkinje cell and molecular layers of BM-MSC-transplanted NP-C mice compared with those in NIH 3T3 cell-transplanted and sham-transplanted NP-C mice, thereby suggesting that BM-MSC transplantation can lead to improved pathological outcomes. It should be noted, however, that such improvement appears limited since there was still some accumulation of both lipids in some Purkinje cells and cells in the granule layer.

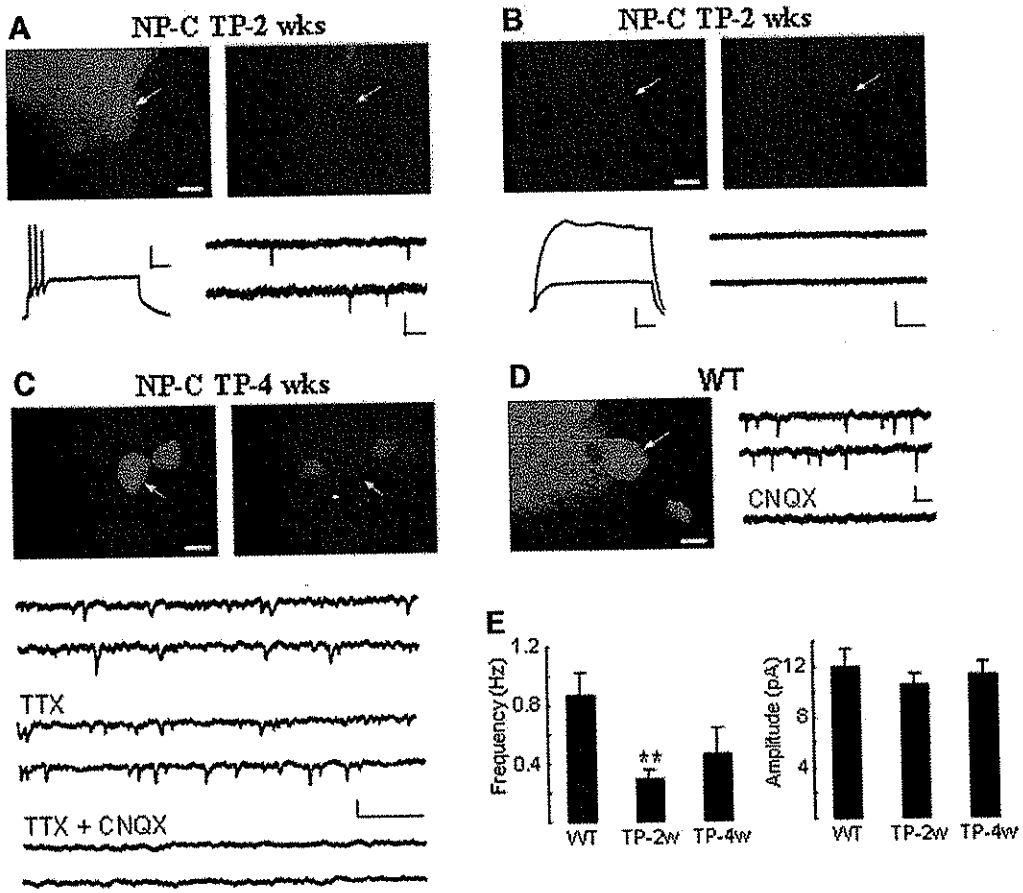

Figure 3. Electrophysiological properties of surviving Purkinje neurons in bone marrow-derived MSC (BM-MSC)-transplanted NP-C $Gsbs^{GFP/+}$ mice. **(A, B):** A Purkinje neuron in a parasagittal slice of cerebellum (lobe IV–VI) obtained from NP-C $Gsbs^{GFP/+}$ mice at TP-2wks **(A)** was labeled with both green fluorescent protein and dsRed. The neuron produced action potential firings by intracellular current injection in current clamp (lower left), and spontaneous excitatory postsynaptic currents (sEPSCs) in voltage clamp were recorded in the neuron (lower right). However, a cell labeled with only dsRed **(B)** did not show action potential firing (lower left) and sEPSC (lower right). **(C, D):** sEPSCs recorded in NP-C $Gsbs^{GFP/+}$ mice at TP-4wks were frequent in normal Krebs solution and in the presence of TTX (1 μM), a voltage-dependent Na^+ channel blocker. The sEPSCs were blocked by CNQX (10 μM), an α-amino-3-hydroxy-5-methyl-4-isoxazolepropionic acid/kainate receptor antagonist, as in the BALB/c $Gsbs^{GFP/+}$ (WT) Purkinje neuron **(D)**. **(E):** Histograms summarize averaged frequencies and amplitudes of sEPSCs recorded in Purkinje neurons obtained from three WT, four TP-2wk, and two TP-4wk mice. The mean frequency of sEPSCs in TP-2wk mice, but not TP-4wk mice, was significantly decreased compared with that in WT mice (*, $p < .01$), whereas the mean amplitudes of sEPSCs were similar among groups. In all photographs, scale bars = 10 μm, and arrows indicate the recorded Purkinje neuron. *x*-axis and *y*-axis, respectively, 50 milliseconds and 20 mV in current clamp; *x*-axis and *y*-axis, 1 second and 20 pA in voltage clamp. Abbreviations: CNQX, 6-cyano-7-nitroquinoxaline-2,3-dione; NP-C, Niemann-Pick disease type C; TP-2wk, 2 weeks after BM-MSC transplantation; TP-4wk, 4 weeks after BM-MSC transplantation; TTX, tetrodotoxin; WT, wild-type.

DISCUSSION

We have recently demonstrated that neurodegeneration augments the ability of BM-MSCs to fuse with Purkinje neurons in NP-C mice following transplantation [13]. An intriguing and potentially important finding in our previous study is that the competence of Purkinje neurons to fuse with donor-derived BM-MSC appears to be upregulated in the NP-C brain, although the mechanism underlying BM-MSC fusion itself remains elusive. In the present study, we have elucidated, by molecular and functional criteria, that BM-MSCs retain the potential to develop into functional CNS neurons when they undergo fusion-like events in neurodegenerative environments. Our findings also show that surviving Purkinje neurons, originating from BM-MSC/Purkinje neuron fusion-like events, develop into electrically active neurons with functional synaptic formation.

The NP-C mouse (a model of human Niemann-Pick disease type C1, an inherited lysosomal storage disorder) is characterized by progressive ataxia, cerebellar atrophy, psychomotor deterioration, extrapyramidal deficits, and dementia [22]. NP-C mice become symptomatic between 6 and 7 weeks, neuronal and glial changes are seen before 6 weeks [38, 39], and behavioral tests show impaired neurological function as early as 28 days [40]. The location of neurotransmitter deficits in the cerebellum and cortex of NP-C mice, including downregulation of glutamate and GABA, correlated with some of the degenerative neuropathology [35]. Therefore, NP-C mice represent an appropriate experimental paradigm for transplantation strategies in which to test the potential of BM-MSC progeny to develop into functional and mature neurons that restore brain function.

In an effort to identify differential gene expression in neurodegenerative mice undergoing BM-MSC transplantation, we carried out gene expression analyses of brain in BM-MSC-transplanted and control NP-C mice. Importantly, our microarray results revealed a dramatically increased level of transcripts

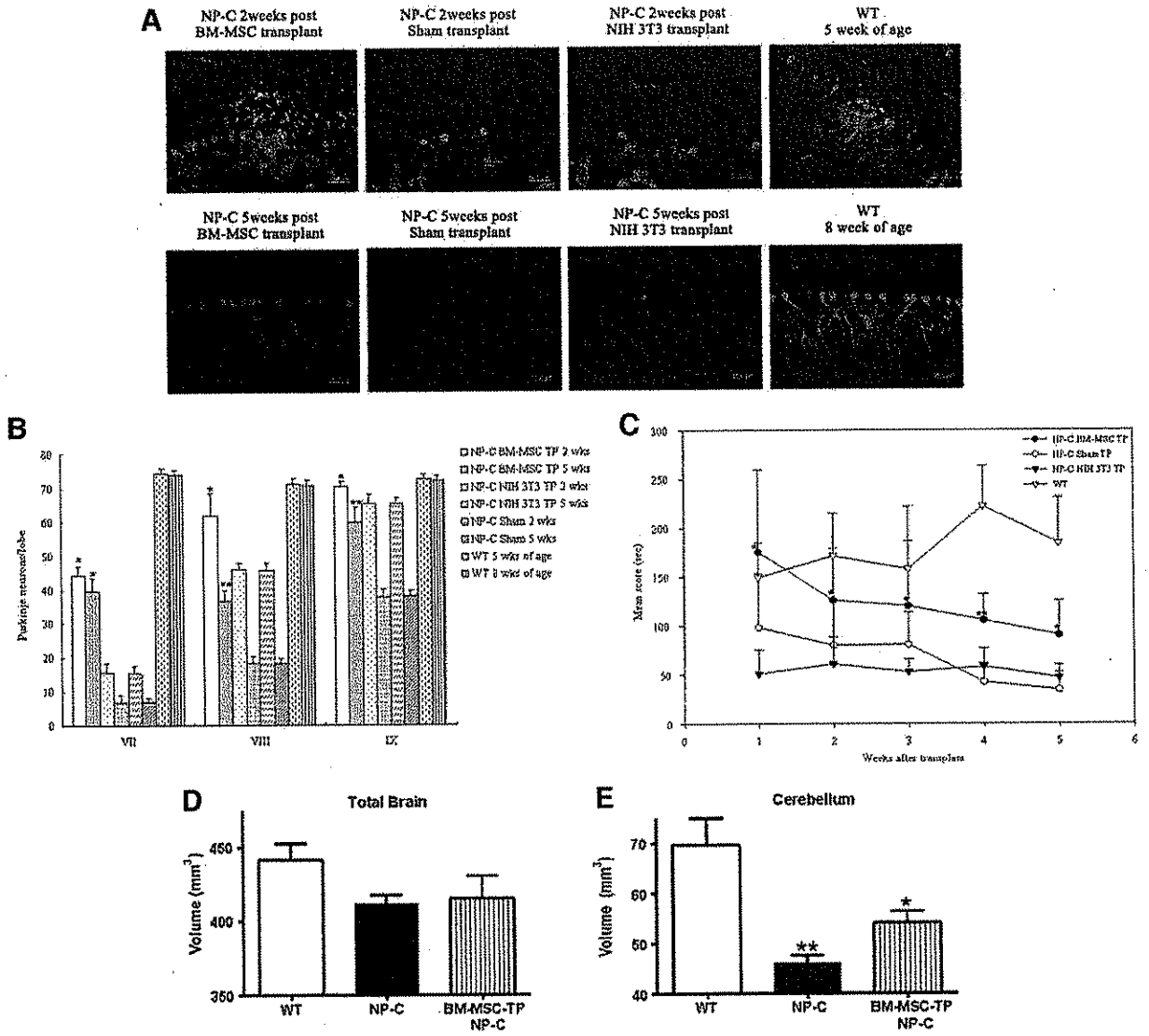

Figure 4. Effect of BM-MSC transplantation on Purkinje neurons in cerebellum. **(A):** Purkinje neuron immunofluorescence staining at 2 and 5 wks after transplantation. Visualization of Purkinje neurons was performed using anti-calbindin antibodies, as described in Materials and Methods. Scale bar = 50 μm. **(B):** Quantification of Purkinje neurons in lobes VII, VIII, and IX of cerebellar vermis in TP and normal NP-C mice. Data are mean ± SEM (n = 6 brains and n = 30 sections in each group). The number of Purkinje neurons was increased significantly in BM-MSC TP NP-C mice. *, $p < .0001$ compared with NP-C NIH 3T3 TP and NP-C sham TP. **, $p < .0001$ compared with NP-C sham TP. **(C):** Rota-Rod scores for TP and control NP-C mice. Rota-Rod scores of individual BM-MSC-TP (filled circles), sham-TP (open circles), NIH 3T3 cell-TP (filled triangles), and normal mice (open triangles) were averaged and plotted beginning 1 week after transplantation (4 wks of age). All of the sham-TP NP-C mice died by 9 wks of age (n = 7 in each group). *, $p < .05$ compared with sham and/or NIH 3T3 transplantation. **, $p < .001$ compared with sham and NIH 3T3 transplantation. **(D, E):** Volumetric ex vivo magnetic resonance imaging measurements (n = 3 in each group). Total brain volume in animals with NP-C (BM-MSC TP and sham-TP NP-C) showed a nonsignificant 10% smaller brain volume compared with normal mice (WT) **(D)**. Both BM-MSC-TP and sham-TP mice showed significantly smaller cerebellar volumes compared with WT. BM-MSC TP NP-C showed a slight attenuation of cerebellar atrophy compared with sham-TP mice. *, $p < .05$; **, $p < .01$ compared with WT mice (E). Abbreviations: BM-MSC, bone marrow-derived MSC; NP-C, Niemann-Pick disease type C; TP, transplanted; wks, weeks; WT, wild-type.

encoding several synaptic proteins, including glutamate and GABA receptor subtypes. The AMPA receptor family of glutamate receptors mediates fast neurotransmission at most excitatory synapses in the brain. The function and expression of AMPA receptors are regulated by composition of the subunits GluR1, 2, 3, and 4. Among the four subtypes of AMPA receptors, GluR1 and GluR4 play a key role in synaptic plasticity in the brain [41]. We observed upregulation of GluR4, $GABA_A$ receptor $\beta 2$, GAD, and MBP, although only GluR4 could be confirmed in protein expression analysis in BM-MSC-transplanted NP-C. This result suggests that BM-MSC transplantation may promote synaptic transmission via AMPA receptor upregulation in this neurodegenerative environment.

One of the hallmarks of mature CNS neurons is their ability to form synapses. Synapses are key structures in the neuronal network, so the functional state of the network is reflected in the formation, rearrangement, degeneration, and regeneration of the synapse [42]. Excitatory glutamate receptors are expressed on Purkinje neurons, and glutamate is used by fibers that convey information from the granule to the Purkinje neurons [36].

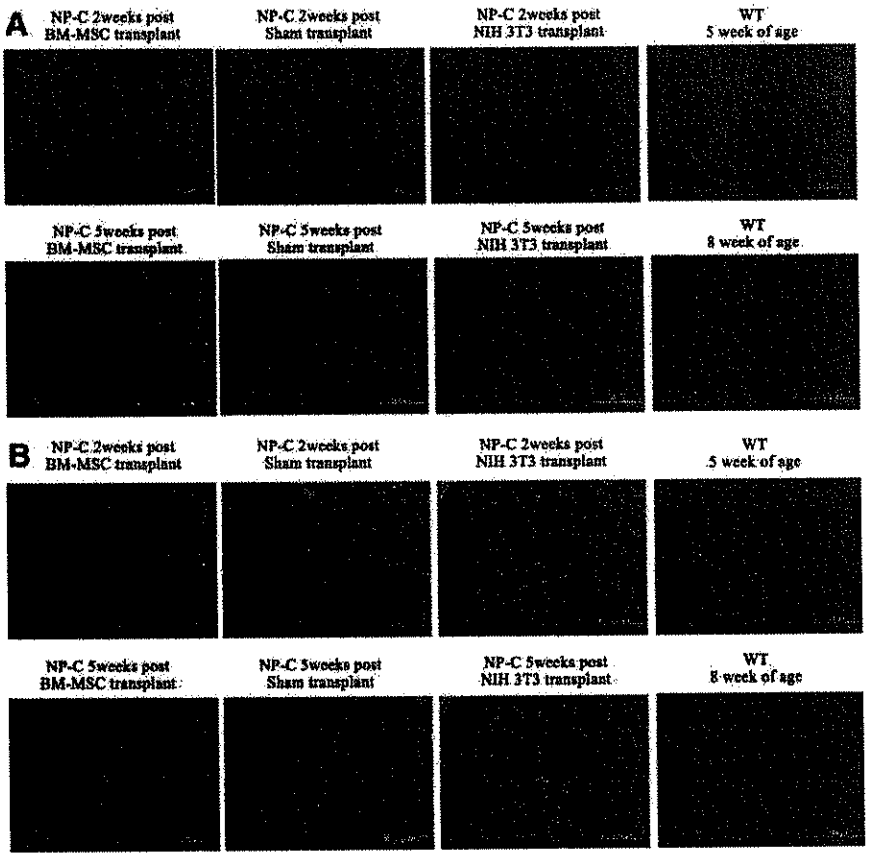

Figure 5. Improved cholesterol and sphingomyelin storage in the cerebellum of BM-MSC-transplanted NP-C mice ($n = 6$ in each group). **(A):** Filipin was used to detect cholesterol in cerebellar sections of transplanted and control NP-C mice. Note that strong positive signals (blue) seen in NIH 3T3 cell-transplanted and sham-transplanted NP-C mice were markedly reduced in BM-MSC-transplanted NP-C cerebellum. **(B):** Lysenin and its polyclonal antibody were used to detect sphingomyelin in cerebellar sections from transplanted and control NP-C mice according to our previous report [12]. Note that reduced signals for lysenin were seen in some Purkinje cells of BM-MSC-transplanted NP-C mice. Scale bar = 50 μm. Abbreviations: BM-MSC, bone marrow-derived MSC; NP-C, Niemann-Pick disease type C; WT, wild-type.

Moreover, glutamate receptors are involved in neuronal differentiation, cell migration, and synaptogenesis in the developing brain [43]. In the present study, BM-MSC transplantation significantly increased the number of surviving Purkinje neurons in NP-C mice, and whole-cell patch-clamp recordings from BM-MSC-transplanted NP-C *Gsbs*$^{GFP/+}$ mice confirmed that many surviving GFP/DsRed-positive Purkinje neurons develop into electrically active Purkinje neurons with functional synaptic formation. Intriguingly, we also found that the DsRed-positive Purkinje neurons, presumably derived from donor-derived BM-MSCs by differentiation, had no action potential firing in current clamp and no sEPSC in voltage clamp (Fig. 3). These data suggest that cell fusion-like events involving BM-MSCs/Purkinje neurons can result in regeneration of synapse formation in the NP-C cerebellum, but they do not elucidate whether BM-MSCs have the capacity to transdifferentiate into Purkinje neurons. Also, improving synaptic function in the cerebellum presumably may mediate the improvement in cerebellar function on Rota-Rod testing (i.e., coordination and balance are improved). Although in the present study we demonstrated that surviving Purkinje neurons had synaptic inputs mediated by AMPA receptors, it would be interesting, as an additional study, to test whether electrical stimulation of afferent fibers (parallel fibers and climbing fibers) in the cerebellum is able to evoke excitatory synaptic currents in the surviving (transplanted) Purkinje neurons. Our findings are supported by those of Song et al., who demonstrated that neural stem cells isolated from adult rat hippocampus develop into electrically active neurons and integrate into neuronal networks with functional synaptic transmission, although that study was performed in vitro [21].

In this study, we have demonstrated—by molecular, structural, and functional criteria—that BM-MSCs retain the potential to develop into functional CNS neurons when transplanted a neurodegenerative environment. In conclusion, our results provide the first direct evidence that functional neurogenesis from BM-MSCs is possible following a fusion-like event with existing Purkinje neurons within a neurodegenerative environment. Furthermore, BM-MSCs, like those derived from embryonic tissues, retain the potential to differentiate into functional neurons with essential properties of mature CNS neurons.

ACKNOWLEDGMENTS

This work was supported by Korea Science and Engineering Foundation Grant M6050100000206A010000210 funded by the Korean government (Ministry of Science & Technology; to H.K.J.) and Korea Research Foundation Grant KRF-2004-015-E00239 funded by the Korean government (Ministry of Education & Human Resources Development, Basic Research Promotion Fund; to H.K.J). In addition, it was partially supported by Regional Technology Innovation Program of the Ministry of Commerce, Industry and Energy Grant RTI04-01-01 (to H.S.H.).

DISCLOSURE OF POTENTIAL CONFLICTS OF INTEREST

The authors indicate no potential conflict of interest.

REFERENCES

1 Azizi SA, Stokes D, Augelli BJ et al. Engraftment and migration of human bone marrow stromal cells implanted in the brains of albino rats similarities to astrocyte grafts. Proc Natl Acad Sci U S A 1998;95:3908–3913.
2 Jiang Y, Jahagirdar BN, Reinhardt RL et al. Pluripotency of mesenchymal stem cells derived from adult marrow. Nature 2002;418:41–49.
3 Kopen GC, Prockop DJ, Phinney DG. Marrow stromal cells migrate throughout forebrain and cerebellum, and they differentiate into astrocytes after injection into neonatal mouse brains. Proc Natl Acad Sci U S A 1999;96:10711–10716.
4 Sanchez-Ramos J, Song S, Cardozo-Pelaez F et al. Adult bone marrow stromal cells differentiate into neural cells in vitro. Exp Neurol 2000; 164:247–256.
5 Woodbury D, Schwarz EJ, Prockop DJ et al. Adult rat and human bone marrow stromal cells differentiate into neurons. J Neurosci Res 2000; 61:364–370.
6 Prockop DJ. Marrow stromal cells as stem cells for nonhematopoietic tissues. Science 1997;276:71–74.
7 Pereira RF, O'Hara MD, Laptev AV et al. Marrow stromal cells as a source of progenitor cells for nonhematopoietic tissues in transgenic mice with a phenotype of osteogenesis imperfecta. Proc Natl Acad Sci U S A 1998;95:1142–1147.
8 Weissman IL, Anderson DJ, Gage F. Stem and progenitor cells: Origins, phenotypes, lineage commitments, and transdifferentiations. Annu Rev Cell Dev Biol 2001;17:387–403.
9 Weimann J, Charlton CA, Brazelton TR et al. Contribution of transplanted bone marrow cells to Purkinje neurons in human adult brains. Proc Natl Acad Sci U S A 2003;100:2088–2093.
10 Alvarez-Dolado M, Pardal MR, Garcia-Verdugo JM et al. Fusion of bone-marrow-derived cells with Purkinje neurons, cardiomyocytes and hepatocytes. Nature 2003;425:968–973.
11 Jin HK, Carter JE, Huntley GW et al. Intracerebral transplantation of mesenchymal stem cells into acid sphingomyelinase-deficient mice delays the onset of neurological abnormalities and extends their life span. J Clin Invest 2002;109:1183–1191.
12 Jin HK, Schuchman EH. Ex vivo gene therapy using bone marrow-derived cells: Combined effects of intracerebral and intravenous transplantation in a mouse model of Niemann-Pick disease. Mol Ther 2003; 8:876–885.
13 Bae JS, Furuya S, Shinoda Y et al. Neurodegeneration augments the ability of bone marrow-derived mesenchymal stem cells to fuse with Purkinje neurons in Niemann-Pick type C mice. Hum Gene Ther 2005; 16:1006–1011.
14 Gage FH. Mammalian neural stem cells. Science 2000;287:1433–1438.
15 Weimann J, Johansson CB, Trejo A et al. Stable reprogrammed heterokaryons form spontaneously in Purkinje neurons after bone marrow transplant. Nat Cell Biol 2003;5:959–966.
16 Palmer TD, Markakis EA, Willhoite AR et al. Fibroblast growth factor-2 activates a latent neurogenic program in neural stem cells from diverse regions of the adult CNS. J Neurosci 1999;19:8487–8497.
17 Brazelton TR, Rossi FM, Keshet GI et al. From marrow to brain: Expression of neuronal phenotypes in adult mice. Science 2000;290: 1775–1779.
18 Mezey E, Chandross KJ, Harta G et al. Turning blood into brain: Cells bearing neuronal antigens generated in vivo from bone marrow. Science 2000;290:1779–1782.
19 Kondo T, Raff M. Oligodendrocyte precursor cells reprogrammed to become multipotential CNS stem cells. Science 2000;289:1754–1757.
20 Roy NS, Wang S, Jiang L et al. In vitro neurogenesis by progenitor cells isolated from the adult human hippocampus. Nat Med 2000;6:271–277.
21 Song HJ, Stevens CF, Gage FH. Neural stem cells from adult hippocampus develop essential properties of functional CNS neurons. Nat Neurosci 2002;5:438–445.
22 Tanaka J, Nakamura H, Miyawaki S. Cerebellar involvement in murine sphingomyelinosis: A new model of Niemann-Pick disease. J Neuropathol Exp Neurol 1988;47:291–300.
23 Loftus SK, Morris JA, Carstea ED et al. Murine model of Niemann-Pick C disease: Mutation in a cholesterol homeostasis gene. Science 1997; 277:232–235.
24 Endo S, Suzuki M, Sumi M et al. Molecular identification of human G-substrate, a possible downstream component of the cGMP-dependent protein kinase cascade in cerebellar Purkinje cells. Proc Natl Acad Sci U S A 1999;96:2467–2472.
25 Li C, Wong WH. Model-based analysis of oligonucleotide arrays: Expression index computation and outlier detection. Proc Natl Acad Sci U S A 2001;98:31–36.
26 Dahlquist KD, Salomonis N, Vranizan K et al. GenMAPP, a new tool for viewing and analyzing microarray data on biological pathways. Nat Genet 2002;31:19–20.
27 Gene Map Annotator and Pathway Profiler. Available at http://www.genmapp.org. Accessed September 4, 2006.
28 von Boyen GB, Steinkamp M, Adler G et al. Glutamate receptor subunit expression in primary enteric glia cultures. J Recept Signal Transduct Res 2006;26:329–336.
29 Linnemann C, Schmeh I, Thier P et al. Transient change in GABA(A) receptor subunit mRNA expression in Lurcher cerebellar nuclei during Purkinje cell degeneration. BMC Neurosci 2006;7:59.
30 Naka F, Narita N, Okado N et al. Modification of AMPA receptor properties following environmental enrichment. Brain Dev 2005;27: 275–278.
31 Kobayashi T, Beuchat MH, Lindsay M et al. Late endosomal membranes rich in lysobisphosphatidic acid regulate cholesterol transport. Nat Cell Biol 1999;1:113–118.
32 Yamaji A, Sekizawa Y, Emoto K et al. Lysenin, a novel sphingomyelin-specific binding protein. J Biol Chem 1998;273:5300–5306.
33 Dunham NW, Miya TS. A note on a simple apparatus for detecting neurological deficit in rats and mice. J Am Pharm Assoc Am Pharm Assoc (Baltim) 1957;46:208–209.
34 Jones BJ, Roberts DJ. The quantitative measurement of motor incoordination in naive mice using an accelerating Rota-Rod. J Pharm Pharmacol 1968;20:302–304.
35 Yadid G, Sotnik-Barkai I, Tornatore C et al. Neurochemical alterations in the cerebellum of a murine model of Niemann-Pick type C disease. Brain Res 1998;799:250–256.
36 Dupont JL, Fourcaudot E, Beekenkamp H et al. Synaptic organization of the mouse cerebellar cortex in organotypic slice cultures. Cerebellum 2006;5:243–256.
37 Sonnewald U, Kortner TM, Qu H et al. Demonstration of extensive GABA synthesis in the small population of GAD positive neurons in cerebellar cultures by the use of pharmacological tools. Neurochem Int 2006;48:572–578.
38 Ong WY, Kumar U, Switzer RC et al. Neurodegeneration in Niemann-Pick type C disease mice. Exp Brain Res 2001;141:218–231.
39 German DC, Quintero EM, Liang CL et al. Selective neurodegeneration, without neurofibrillary tangles, in a mouse model of Niemann-Pick C disease. J Comp Neurol 2001;433:415–425.
40 Võikar V, Koks S, Vasar E et al. Strain and gender differences in the behavior of mouse lines commonly used in transgenic studies. Physiol Behav 2001;72:271–281.
41 Borges K, Myers SJ, Zhang S et al. Activity of the rat GluR4 promoter in transfected cortical neurons and glia. J Neurochem 2003;86: 1162–1173.
42 Garner CC, Zhai RG, Gundelfinger ED et al. Molecular mechanisms of CNS synaptogenesis. Trends Neurosci 2002;25:243–250.
43 Komuro H, Rakic P. Modulation of neuronal migration by NMDA receptors. Science 1993;260:95–97.

See www.StemCells.com for supplemental material available online.